

# PHYLOGEOGRAPHIC STRUCTURING WITHIN RECENTLY DIVERGED SCORPION SPECIES, *EUSCORPIUS BOROVLAVAENSIS* TROPEA, 2015 (SCORPIONES, EUSCORPIIDAE), WITH THE DESCRIPTION OF A NEW SUBSPECIES

MARTINA PODNAR\*<sup>1</sup>, VALERIO VIGNOLI<sup>2</sup> & NIKOLA TVRTKOVIĆ<sup>3</sup>

<sup>1</sup>Croatian Natural History Museum, Demetrova 1, 10000 Zagreb, Croatia  
(e-mail: martina.podnar@hpm.hr)

<sup>2</sup>Siena, Italy (e-mail: vignoliv@gmail.com)

<sup>3</sup>Croatian Biospeleological Society, Rooseveltov trg 6, 10000 Zagreb, Croatia  
(e-mail: nikolatvrtkovic71@gmail.com)

**Podnar, M., Vignoli, V. & Tvrtković, N.: Phylogeographic structuring within recently diverged scorpion species, *Euscorpius borovaglavaensis* Tropea, 2015 (Scorpiones: Euscorpiidae) in Croatia, with the description of a new subspecies. Nat. Croat., Vol. 33, No. 1., 29-52, 2024, Zagreb.**

The European scorpion *Euscorpius borovaglavaensis* Tropea, 2015 is a morphologically cryptic species that is distinguishable only with difficulty from *E. tergestinus* (C. L. Koch, 1837). It is distributed in the middle part of the Dinaric Alps chain and along part of the Eastern Adriatic coast, specifically, in Croatia (Middle Dalmatia, Lika karst upland), as well as in the southern part of Bosnia and Herzegovina. The new findings reported here have enhanced our knowledge of its geographic distribution in Croatia. Detailed morphological analyses highlighted the importance of carination in the ventral metasomal segments as morphological traits. Phylogenetic analyses, based on the mitochondrial cytochrome *c* oxidase subunit I (*COI*) gene, have revealed the existence of two distinct lineages. One of them, distributed in the northwestern part of the range, is described here as *E. b. flavus* **n. ssp.**, while the nominal subspecies occurs in the southeastern part. A time-calibrated phylogenetic analysis has established their divergence around 0.9 million years ago, coinciding with the Mid-Pleistocene Transition (MPT) period. In contrast to the nominal subspecies, *E. b. flavus* **n. ssp.** exhibits significant phylogeographic structuring, indicating recent isolation events in multiple glacial microrefugia after the initial divergence, followed by a final Holocene dispersal in the northwestern direction deep between the mountain chains.

**Key words:** Scorpiones, Euscorpiidae, phylogeny, mtCOI gene, taxonomy, Croatia, Bosnia and Herzegovina

**Podnar, M., Vignoli, V. & Tvrtković, N.: Filogeografsko strukturiranje unutar nedavno razdvojenih populacija škorpiona vrste *Euscorpius borovaglavaensis* Tropea, 2015 (Scorpiones: Euscorpiidae) u Hrvatskoj, uz opis nove podvrste. Nat. Croat., Vol. 33, No. 1., 29-52, 2024, Zagreb.**

Europski škorpion *Euscorpius borovaglavaensis* Tropea, 2015 je morfološki kriptična vrsta koja se vrlo teško razlikuje od *E. tergestinus* (C. L. Koch, 1837). Rasprostranjen je u središnjem dijelu lanca Dinarida i dijelu obale Jadrana, u Hrvatskoj (srednja Dalmacija i Lička visoravan) te Bosni i Hercegovini. Novoobjavljeni nalazi upotpunjuju dosad poznato rasprostranjenje u Hrvatskoj. Detaljna analiza morfologije istaknula je važnost uzdužnih izbočina s kvržicama donje strane metasomnalnih članaka kao razlikovnih morfoloških značajki. Filogenetskom analizom COI gena potvrđene su dvije zasebne molekule

---

\*Corresponding author

larne linije. Jedna od njih, ona koja je rasprostranjena sjeverozapadno, opisana je kao *E. b. flavus n. ssp.*, dok nominalnu podvrstu nalazimo u jugoistočnom dijelu rasprostranjenja. Vremenski kalibriranom filogenetičkom analizom procijenjeno je njihovo razdvajanje na prije otprilike 0,9 milijuna godina, što odgovara razdoblju srednjepleistocenskih promjena (MPT). Za razliku od uzoraka nominalne podvrste, uzorci populacija *E. b. flavus n. ssp.* pokazuju značajno filogeografsko strukturiranje. To ukazuje da je nakon početnog razdvajanja genetskih linija došlo do izolacija u više razdvojenih ledenodobnih pribježišta, iz kojih u holocenu slijede naseljavanja u smjeru sjeverozapada, duboko među planinske lance.

**Ključne riječi:** Scorpiones, Euscorpiidae, filogenija, mitohondrijski COI gen, taksonomija, Hrvatska, Bosna i Hercegovina

## INTRODUCTION

*E. borovaglavaensis* Tropea, 2015 was described from Bosnia and Herzegovina by TROPEA (2015) as a new morphologically cryptic species similar to *Euscorpius tergestinus* (C. L. Koch, 1837). The author pointed out that the only way to distinguish these two species is through the different coloration: light brown reddish to yellow in *E. tergestinus* and dark brown with marked marbling on most of the body in *E. borovaglavaensis* Tropea, 2015. He registered the new species in Croatia as well, one specimen near the Adriatic coast east of Split, south of Dubrava, previously identified as *E. tergestinus* (GRAHAM *et al.*, 2012) and additional specimens in a larger sample from Makarska (Coll. MSNB). He noted that *E. tergestinus* inhabits the eastern Adriatic coast from Istria to Split and found this species also in Metković near Neretva River mouth. PODNAR *et al.* (2021) after a broader phylogenetic analysis recognized that two previously published *E. borovaglavaensis* DNA barcode sequences were erroneously associated with *E. tergestinus* (VF-0772) and *E. hadzii* (VF-0808). In the same study, the sample from Šolta Island (Coll. NHMW), formerly recognized as *E. tergestinus* (FET & SOLEGLAD, 2002), clustered within the *E. borovaglavaensis* clade too. Also, the authors provided an enlarged distribution area for *E. borovaglavaensis*. Thereby, the specimens from two localities, Mt. Svilaja in Middle Dalmatia north of Split and Mogorić, more to the northwest, in the Lika region (both Croatia), were not typical in color. The small sample studied was characterized by interestingly high intraspecific distances, probably due to the isolation of populations in several glacial microrefugia. Increased field efforts with newly collected material from Croatia and Bosnia and Herzegovina, enabled and also pointed to the need for taxonomic intraspecific revision as the first step to a broader taxonomic revision (in progress) regarding the whole "*E. tergestinus* group" in Eastern Adriatic.

## MATERIAL AND METHODS

### Morphological Analyses

Specimens are preserved in 75-95% ethyl alcohol. Measurements were taken with an Euromex Z1654 stereomicroscope fitted with a micrometer ocular, recorded in mm and follows TROPEA *et al.* (2014), CAIN *et al.* (2021) for pedipalp chela manus and tergites length, STAHNKE (1970) for carapace anterior length. Geographical coordinates in the field were taken with a portable Garmin GPS device. Coordinates converted with The World Coordinate Converter (TWCC) maps, altitudes from the Croatian samples were taken from ARKOD.preglednik/hr maps. Publications used for morphological terminology are the following: trichobothria nomenclature: VACHON (1974); generic morphology: STAHNKE (1970), HJELLE (1990), SISSOM (1990); carination, leg setation and pedipalp

dentition: GONZÁLEZ-SANTILLIÁN & PRENDINI (2013); chelicerae dentition: SOLEGLAD & SISSOM (2001); sternum terminology: SOLEGLAD & FET (2003); pedipalp chela finger margins: KOVAŘÍK & ŠTÁHLAVSKÝ (2020); lateral ocelli model: LORIA & PRENDINI (2014). Carination and morphosculpture were observed under UV light (VOLSCHEK, 2005). Colors have been determined on preserved specimens using NCS - Natural Colour System<sup>®</sup> (NCS Scandinavian Colour Institute, Stockholm, Sweden) under a 1600 lumen led lamp (5600-6500 K). Images were made under UV and visible light using a Fujifilm X-T2 digital camera equipped with a Laowa 65 mm and a Fujifilm 60 mm lens equipped with Raynox DCR-250 macro lens. The holotype and three paratypes are deposited in the CNHM, other paratypes in MSNT, CNHM, NHMW and MSNB.

Acronyms. **MSNT** = Museo civico di Storia Naturale di Trieste, Italy; **CNHM** = Croatian Natural History Museum (Hrvatski prirodoslovni muzej), Zagreb, Croatia; **MSNB** = Museo Civico di Scienze Naturali E. Caffi, Bergamo, Italy; **NHMW** = Naturhistorisches Museum, Wien; **ZMBH** = Zemaljski muzej Bosne i Hercegovine, Sarajevo, Bosnia and Herzegovina; **VVZC** = Valerio Vignoli Zoological Collection, Siena, Italy; **PMST** = Prirodoslovni muzej Split, Croatia; **RMNH** = Rijksmuseum van Natuurlijke Historie, Leiden, Netherlands; **GTC** – personal collection of Gioele Tropea, Rome, Italy; **HNHM** – Hungarian Natural History Museum Budapest, Hungary; **Lchel** = pedipalp chela length; **Wchel** = pedipalp chela width; **L** = left; **R** = right; **H** = height; **Lfem** = pedipalp femur length; **Lpat** = pedipalp patella length; **Lcar** = carapace length; **Wcar** = carapace width.

The specimens used for description of the new taxon are given in the taxonomic part of the results. For comparative study the following 13 specimens of *E. borovaglavaensis* Tropea, 2015 were examined: 1 adult ♀ (CNHM786), **Borova Glava pass**, Duman Mt. (Krug Mts.), Bosnia and Herzegovina, 43°46'56"N, 17°07'53"E, 24.VII.2022, J. Kasalo, J. Skejo and N. Kasalo leg.; 3 adult ♂♂ (ZMBH76, VVZC1380, VVZC1382), 1 sub adult ♂ (PMST10), 4 adult ♀♀ (VVZC1381, VVZC1379, PMST9, CNHM788), **S Lištani, W Odžak**, Mt. Troglav (Dinara Mts.), Bosnia and Herzegovina, 43°51'40"N, 16°45'28"E, 1160 m a.s.l., 16.VIII.2022, T. Rađa leg.; 1 adult ♀ (CNHM787), **Rože**, Voštane, Mt. Kamešnica, Croatia, 43°51'40"N, 16°45'28"E, 815 m a.s.l., 24.VII.2022, N. Tvrtković leg.; 1 adult ♀ (ZMBH75) **Gornja Bukovica**, Mt. Midena, Bosnia and Herzegovina, 43°36'01"N, 17°15'17"E, 1000 m a.s.l., V. Ljubas leg.; 2 adult ♀♀ (CNHM765, NHMW 29983), **Duler**, Mt. Dinara, 44°05'05"N, 16°21'23"E, 1220 m a.s.l., G. Rnjak leg. Additional samples of *E. tergestinus* (C. L. Koch, 1837), examined for comparison with all *E. borovaglavaensis*: 2 adult ♀♀ (VVZC226, VVZC227), **Trieste**, Friuli Venezia Giulia, Italy, 16.IV.1967, Folco Giusti leg.; 3 adult ♂♂ (VVZC1429-31), 5 adult ♀♀ (VVZC1388, 1432-34, 1436), 1 juvenile (VVZC1437), **Ternova piccola**, Duino-Aurisina, Trieste, Italy, 45°46'03.7"N; 13°43'08.5"E, 301 m a.s.l., 01.XI.2022, V. Vignoli leg.; 1 adult ♀ (VVZC1387), 1 juvenile (VVZC1439), **Bosco Bazzoni**, Basovizza, Trieste, Italy, 45°37'44.8"N; 13°52'05.6"E, 387 m a.s.l., 01.XI.2022, V. Vignoli leg.; 1 adult ♀ (VVZC1440), after Bosco Bazzoni, Basovizza, Trieste, Italy, 45°37'40.4"N; 13°52'40.1"E, 406 m a.s.l., 01.XI.2022, V. Vignoli leg., together with 20 more *E. tergestinus* specimens collected in Italy and Croatia preserved in MSTN and published in TROPEA (2013a) including neotype: 1 adult ♂ (SC18-4001), Sito 2L-UTM, **Hotel Pesek, Basovizza**, Trieste, Friuli Venezia Giulia, Italy, 450 m a.s.l., 16.IX.2005, A. Quadracci leg.; and Croatian coastal *E. tergestinus* specimens preserved in CNHM (PODARN *et al.*, 2021).

## Molecular Analyses

### DNA extraction, PCR amplification and sequencing

Total genomic DNA was extracted from a single leg of each individual specimen using the GenElute Mammalian Genomic DNA Miniprep Kit (Sigma) following the manufacturer's instructions and eluted in 100  $\mu$ l of Elution Solution. A partial region of the mitochondrial (mt) *cytochrome c oxidase subunit 1* gene (*COI*, the DNA barcode region, HEBERT *et al.*, 2003) was amplified from 18 specimens (Tab. 1a and 1b, Fig. 1) using PCR primers and under the conditions given in PODNAR *et al.* (2021). Sequencing of PCR products using amplification primers was conducted at Macrogen Europe sequencing services (Amsterdam, The Netherlands), and sequences are deposited in BOLD (<http://www.boldsystems.org/>; RATNASINGHAM & HEBERT, 2007).

### Sequence editing, alignment and distance analysis

Sequences were inspected, edited and aligned with the use of BioEdit v. 7.2.5. (HALL, 1999). The ranges of intra- and inter-clade uncorrected pairwise distances (p-distances) for *COI* sequences were calculated with MEGA version 11 (TAMURA *et al.*, 2021). Along with the 18 newly obtained sequences (Tab. 1a and 1b), the data set consisted of all previously published full-length DNA barcodes of *Euscorpium borovaglavaensis*, *E. tergestinus* and *E. cf. tergestinus*, which were retrieved from BOLD.

### Population dynamics and phylogenetic analyses

A time-calibrated Bayesian tree based on the *COI* sequences listed in Tab. 1a and 1b was estimated using BEAST version 2.7.3 (BOUCKAERT *et al.*, 2019) available at CIPRES Science Gateway (MILLER *et al.*, 2010). The sequences of *E. feti* were used as outgroups. Prior to analysis, the best-fit model of nucleotide substitution (GTR+G) was assessed with jModelTest version 2.1.6 (DARRIBA *et al.*, 2012) on XSEDE under Bayesian information criteria, also through the CIPRES gateway, and the molecular clock test was performed in MEGA version 11 (TAMURA *et al.*, 2021) to determine whether the rates of molecular evolution vary significantly among the lineages. Since the molecular clock hypothesis has not been rejected, the strict molecular clock with a fix rate of nucleotide substitutions set to 0.0134 (95% HPD: 0.01–0.0174) substitutions/site/million years (PODNAR *et al.*, 2021) was applied. The analysis was run for 30,000,000 generations, sampling every 3000th generation, and the first 10% of the sampled trees were discarded as burn-in. The convergence of runs and effective sample size (ESS) values were checked by Tracer v1.7.2. (RAMBAUT *et al.*, 2018) and the maximum clade credibility tree was constructed using TreeAnnotator v.2.7.3 (included in the BEAST 2.7.3. package) and visualized in FigTree v.1.4.4 (<http://tree.bio.ed.ac.uk>) software.

The 95% statistical parsimony (TCS) haplotype network (TEMPLETON *et al.*, 1992) of all available *E. borovaglavaensis* complete DNA barcode region sequences (Tab. 1.a) was constructed with the use of PopART v. 1.7 (LEIGH & BRYANT, 2015) software. Finally, the Bayesian skyline plots (BSPs) were constructed to contrast the past demographic history of the two main *E. borovaglavaensis* lineages using BEAST version 2.7.3 (BOUCKAERT *et al.*, 2019) package. The optimal model of sequence evolution, HKY for both lineages, was selected in MEGA version 11 (TAMURA *et al.*, 2021) using Bayesian information criteria. The strict molecular clock model with the same evolutionary rate as implemented in the BEAST divergence dating analysis (see above) and Bayesian skyline coalescent tree prior (DRUMMOND *et al.*, 2005) were employed. The Markov Chain Monte Carlo (MCMC) chain length was set to 10,000,000 generations with a sampling fre-

**Tab. 1a.** List of *Euscorpium borovaglavaensis* specimens used in the molecular part of the study and in the distribution maps. The number in column 3 refers to the numbers presented on maps in Fig. 1. Sample codes (ID), locality, Collection inventory numbers (ID; CNHM - Croatian Natural History Museum, Scorpiones and Pseudoscorpiones Collection; NHMW - Natural History Museum Vienna, MU - Marshall University; VVZC - Valerio Vignoli Zoological Collection), BOLD (COI; DNA barcode region) accession numbers, COI sequence haplotype (H1-12) and reference are given. Abbreviations: HR = Croatia, BIH = Bosnia and Herzegovina, I = Italy, Ref = references: A = PODNAR *et al.* (2021), B = GRAHAM *et al.* (2012b), C = present study, D = TROPEA (2015), E = iBOL.

| Sample ID                          | Locality (short version)                  | No. | Voucher ID   | COI accession numbers | COI Hp | Ref |
|------------------------------------|---|-----|--------------|-----------------------|--------|-----|
| <i>Euscorpium borovaglavaensis</i> |   |     |              |                       |        |     |
| S6                                 | HR: Split ?                               | 1   | NHMW_11744   | ATCRO013-21           | H1     | A   |
| VF-0808                            | SRB: Niš                                  | -   | MU_VF-0808-1 | AMSCO067-10           | -      | E   |
| VF-0772                            | HR: 10 km E of Split, 0.5 km S of Dubrava | 2   | MU_VF-0772-1 | AMSCO046-10           | H2     | B   |
| CROB1425                           | BIH: Gornja Bukovica                      | 3   | ZMBH 75      | CROSB001-23           | H3     | C   |
| CROB613                            | BIH: Cebara, Tomislavgrad                 | 4   | CNHM_391     | CROSC034-21           | H4     | A   |
| CROB1424                           | BIH: Borova Glava pass                    | 5   | CNHM_786     | CROSB002-23           | H4     | C   |
| CROB1396                           | BIH: Lištani - Odžak                      | 6   | CNHM_788     | CROSB003-23           | H4     | C   |
| CROB1395                           | HR: Rože, Voštane                         | 7   | CNHM_787     | CROSB004-23           | H4     | C   |
| CROB1423                           | HR: Duler, Dinara Mt.                     | 8   | CNHM 765     | CROSB005-23           | H4     | C   |
| -                                  | BIH: Barevo                               | 9   | MSNB 8771    | -                     |        | D   |
| -                                  | BIH: Nevesinje, Luka                      | 10  | RMNH         | -                     |        | D   |
| -                                  | BIH: Prisoje, Buško jezero lake           | 11  | GTC          | -                     |        | D   |
| -                                  | BIH: Jablanica                            | 12  | HNHM         | -                     |        | D   |
| -                                  | HR: Makarska                              | 13  | MSNB         | -                     |        | D   |
| S23                                | HR: Šolta island                          | 14  | NHMW_2162    | ATCRO012-21           | H6     | A   |
| CROB1138                           | HR: Rađeni, Maljkovo                      | 15  | CNHM_782     | CROSB006-23           | H5     | C   |
| CROB1137                           | HR: Ježević, Marini bunari                | 16  | CNHM_783     | CROSB007-23           | H5     | C   |
| CROB1162                           | HR: Prpino brdo, Mazin                    | 17  | CNHM_796     | CROSB008-23           | H5     | C   |
| CROB197                            | HR: Svilaja Mt.                           | 18  | CNHM_267     | CROSC036-21           | H11    | A   |
| CROB1397                           | HR: Simurđići, Klapavica                  | 19  | CNHM_789     | CROSB009-23           | H7     | C   |
| CROB1154                           | HR: Ondić                                 | 20  | CNHM_792     | CROSB010-23           | H7     | C   |
| CROB1164                           | HR: Trnavac, Grahovci                     | 21  | CNHM_790     | CROSB011-23           | H7     | C   |
| CROB1167                           | HR: Mala Plana                            | 22  | CNHM_795     | CROSB012-23           | H7     | C   |
| CROB1422                           | HR: Krasno                                | 23  | CNHM_794     | CROSB013-23           | H7     | C   |
| CROB1165                           | HR: Kik, Lovinac-G. P.                    | 24  | CNHM_791     | CROSB014-23           | H9     | C   |
| CROB1168                           | HR: Simurđići, Klapavica                  | 25  | CNHM_793     | CROSB015-23           | H10    | C   |
| -                                  | HR: Vojvodići, Mazin                      | 26  | PMST 11      | -                     |        |     |
| -                                  | HR: Bjelobabe, Ličko polje                | 27  | NHMW 29981   | -                     |        |     |
| CROB609                            | HR: Mogorić, Ličko polje                  | 28  | CNHM_239     | CROSC035-21           | H8     | A   |
| CROB1140                           | HR: Vrdovo, Troglav Mt.                   | 29  | CNHM_784     | CROSB016-23           | H5     | C   |

quency of every 1000th generation. The first 1,000,000 generations were discarded as a burn-in. Tracer v1.7.2. (RAMBAUT *et al.*, 2018) was then used to check the sufficiency of effective sample size (ESS>200 for all parameters) and to reconstruct Bayesian Skyline plots.

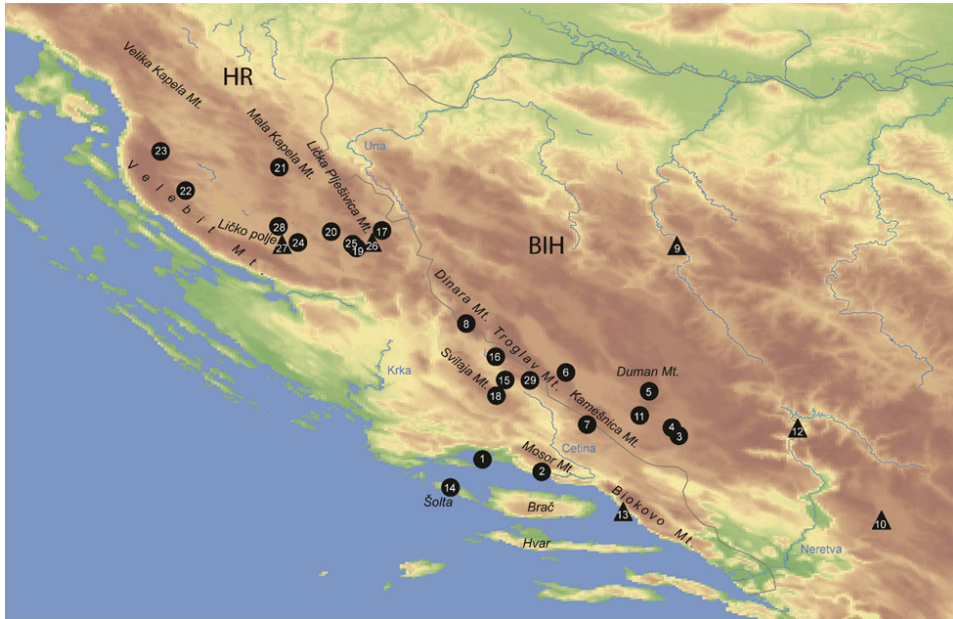


**Fig. 1.** Geographic origin of *Euscorpius borovaglavaensis* Tropea, 2015 specimens analyzed in the present study. Circles on the map represent sampling localities, and the numbers correspond to those listed in Tab.1a. Circles denote DNA barcoded samples. Triangles represent genetically uncharacterized samples from TROPEA (2015) and this study. The sample from Niš, Serbia is not depicted.

**Tab. 1b.** List of other *Euscorpius* specimens used for molecular analysis in the study. Sample codes (ID), locality, Collection inventory numbers (ID; CNHM – Croatian Natural History Museum Scorpiones and Pseudoscorpiones Collection; VVZC – Valerio Vignoli Zoological Collection), BOLD (COI; DNA barcode region) accession numbers; Abbreviations: HR = Croatia, I = Italy, Ref = references: A = PODNAR *et al.*, 2021, C = present.

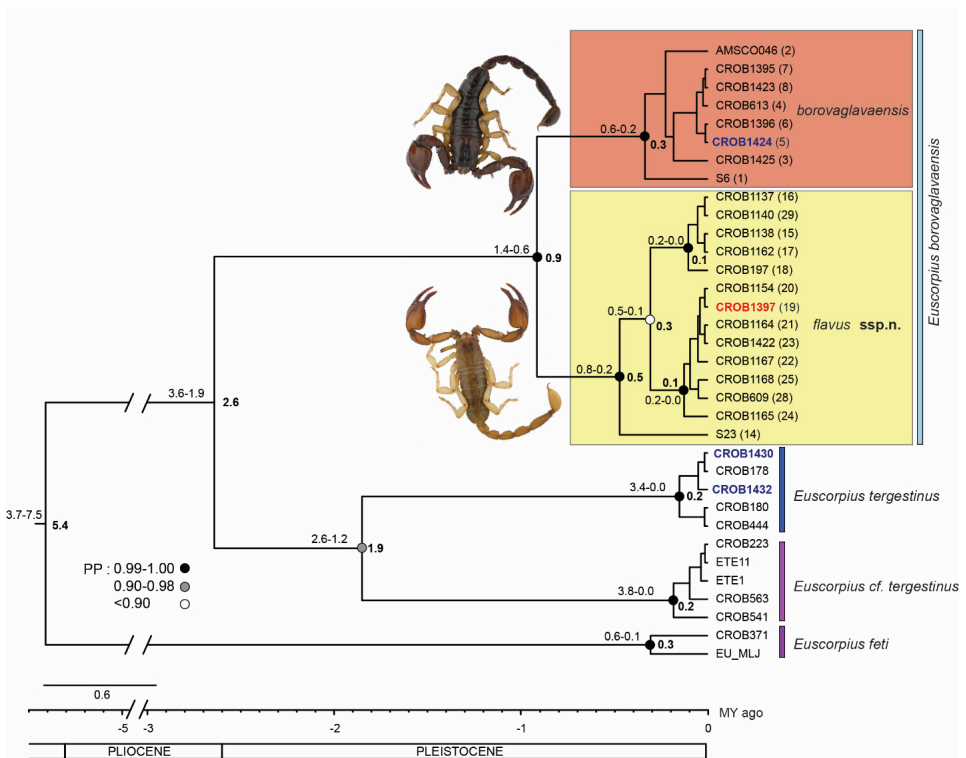
| Sample ID                         | Locality (short version)                 | No. | Voucher ID | COI accession numbers | Ref |
|-----------------------------------|--|-----|------------|-----------------------|-----|
| <i>Euscorpius tergestinus</i>     |  |     |            |                       |     |
| CROB1430                          | I: Basovizza, Trieste (topotype)         | -   | VVZC1387   | CROSB017-23           | C   |
| CROB1432                          | I: Ternova, Trieste                      | -   | VVZC1388   | CROSB018-23           | C   |
| CROB180                           | HR: Baške Oštarije, Mt Velebit           | -   | CNHM_236   | CROSC074-21           | A   |
| CROB444                           | HR: Mandre, island Pag                   | -   | CNHM_323   | CROSC076-21           | A   |
| CROB178                           | HR: Trstenik, Čićarija Mt.               | -   | CNHM_232   | CROSC079-21           | A   |
| <i>Euscorpius cf. tergestinus</i> |  |     |            |                       |     |
| CROB223                           | HR: Rudine - Čižići, island Krk          | -   | CNHM_260   | CROSC082-21           | A   |
| ETE11                             | HR: Sv. Vid Dobrinjski, island Krk       | -   | CNHM_308   | CROSC083-21           | A   |
| CROB563                           | HR: Brgulje, island Molat                | -   | CNHM_347   | CROSC084-21           | A   |
| ETE1                              | HR: islet Supin, Brijuni archipelago     | -   | CNHM_161   | CROSC091-21           | A   |
| CROB541                           | HR: islet Sv. Marko, Brijuni Archipelago | -   | CNHM_343   | CROSC092-21           | A   |
| <i>Euscorpius feti</i>            |  |     |            |                       |     |
| EU-MLJ                            | HR: Galičnjak, cave, island Mljet        | -   | CNHM_321   | CROSC051-21           | A   |
| CROB371                           | HR: Tarina jama, cave, Opuzen            | -   | CNHM_265   | CROSC008-20           | A   |

## RESULTS

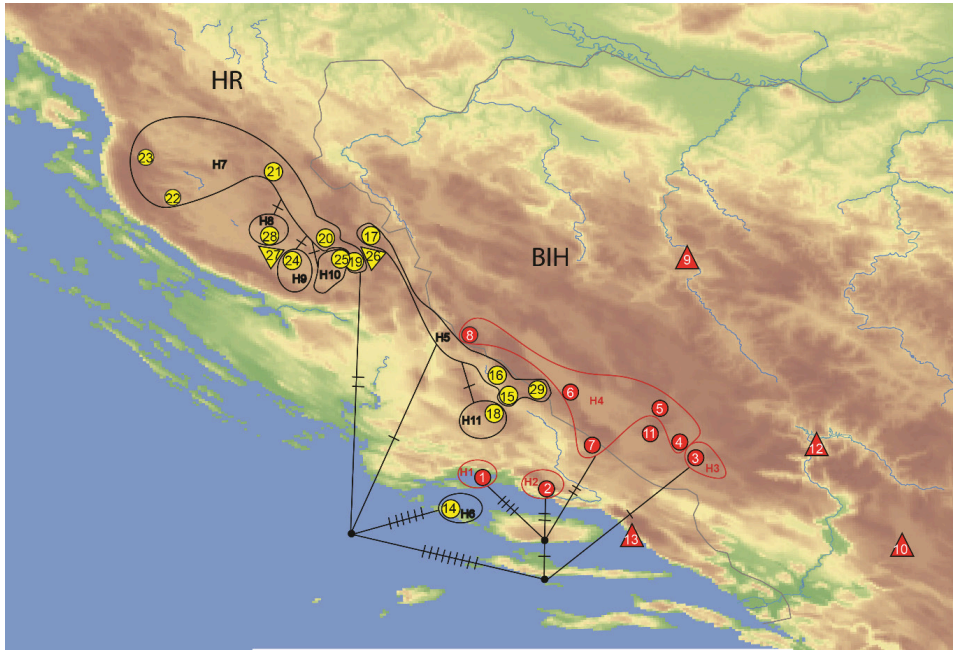
### Phylogeny and phylogeography

All *E. borovaglavaensis* COI sequences clustered within a highly supported monophyletic clade in the time-calibrated Bayesian phylogenetic tree (Fig. 2). This clade is further subdivided into two highly supported monophyletic subclades corresponding to subspecies *E. b. borovaglavaensis* and *E. b. flavus n. ssp.* that diversified 0.9 MYA (95% HPD 1.4-0.6 MYA). Within the *E. b. flavus n. ssp.* subclade, dated to 0.5 (95% HPD 0.8-0.2) MYA, there is additional subdivision into two highly supported lineages plus highly divergent sequence of S6 obtained from the specimen from Šolta Island. Diver-sification of the somewhat younger *E. b. borovaglavaensis* subclade is dated at 0.3 (HPD 0.6-0.2) MYA.

The same phylogenetic relationships are revealed in TCS parsimony network (Fig. 3). Two subspecies are separated by at least 11 mutational steps, and further subdivision also strongly resembles the topology revealed by Bayesian analysis. The species is phylogeographically highly structured, with *E. b. borovaglavaensis* haplotypes in the



**Fig. 2.** Time-calibrated Bayesian phylogenetic tree inferred from COI DNA barcode sequences. The divergence times are depicted as median values and 95% HPD intervals. Circles on nodes represent clade support (Bayesian posterior probabilities, PP). Two separate lineages of *E. borovaglavaensis*, *E. b. borovaglavaensis* and *E. b. flavus n. ssp.* are depicted in red and yellow color, respectively. The topotype specimens are marked in blue and the holotype specimen is indicated in red.

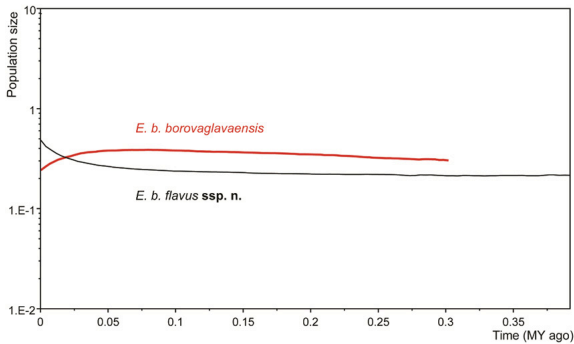


**Fig. 3.** Geographic distribution of *COI* lineages and haplotypes as well as the TCS haplotype network illustrating the relationship between 11 observed *COI* haplotypes. Circles and triangles on the map represent sampling localities, and the numbers correspond to those listed in Tab. 1a. Circles denote DNA barcoded samples. Two separate lineages, *E. b. borovaglavaensis* and *E. b. flavus n. ssp.* are depicted in red and yellow color, respectively. In TCS haplotype network, *E. b. borovaglavaensis* and *E. b. flavus n. ssp.* haplotypes are depicted in red and black color, respectively, and the number of mutational steps is indicated by the number of dashes along the branches. Abbreviations: BIH = Bosnia and Herzegovina, HR = Croatia.

south-east, and *E. b. flavus n. ssp.* haplotypes in the north-west part of the range (Fig. 3). The geographically closest samples belonging to different subspecies are separated either by the high-altitude (> 1300 m a.s.l.) Troglav-Dinara chain (*E. b. flavus n. ssp.* haplotype H5 from *E. b. borovaglavaensis* haplotype H4) or by the sea (*E. b. flavus n. ssp.* haplotype H6 from *E. b. borovaglavaensis* haplotypes H1 and H2). Despite the small genetic divergence (a minimum distance of three mutational steps), the phylogeographic structuring is clearly seen also in the distribution of two mainland *E. b. flavus n. ssp.* sublineages, one of them occupying exclusively the northern part (Haplotypes H7-H10), and the other, with a single exception (Locality 17, Haplotype H5), mostly the southern part of the subspecies range. Bayesian sky plot analysis revealed a somewhat different time to the most recent common ancestor (tMRCA) for two subspecies, the shorter for *E. b. borovaglavaensis* (~ 0.3 MYA) and ~ 0.4 MYA for *E. b. flavus n. ssp.* Another marked difference in the demographic pattern observed is that the population of *E. b. flavus n. ssp.* slightly increased and the population of *E. b. borovaglavaensis* slightly declined in the last 50.000 years. The uncorrected pairwise genetic distances observed between the two subspecies (1.7-2.3%) do not overlap with those found within each of them (Tab. 2).

**Tab. 2.** Ranges of intra- and interspecific uncorrected pairwise genetic distances (p-distances; in percentages) based on DNA barcode fragment of the COI gene.

|   | <i>E. b. borovaglavaensis</i> | <i>E. b. flavus</i> n. ssp. | <i>E. tergestinus</i> | <i>E. cf. tergestinus</i> |
|---|-------------------------------|-----------------------------|-----------------------|---------------------------|
| <i>Euscorpius borovaglavaensis borovaglavaensis</i> | 0.6-0.9                       |                             |                       |                           |
| <i>Euscorpius borovaglavaensis flavus</i> n. ssp.   | 1.7-2.3                       | 0.2-1.4                     |                       |                           |
| <i>Euscorpius tergestinus</i>                       | 4.8-5.7                       | 4.8-5.7                     | 0.3                   |                           |
| <i>Euscorpius cf. tergestinus</i>                   | 4.9-6.2                       | 4.5-6.3                     | 3.9-4.9               | 0.2-1.7                   |

**Fig. 4.** Bayesian skyline plots (BSPs) for subspecies of *E. borovaglavaensis* illustrating population size change through time assuming the COI substitution rate of 0.0134 (95% HPD: 0.01–0.0174) substitutions/site/million years. Only median estimates are shown. The x-axis is a time from the present in MY, and y-axis represents population size (shown on a log scale as the product of the effective population size ( $N_e$ ) and generation time ( $T$ )). *E. b. borovaglavaensis* and *E. b. flavus* n. ssp. are depicted in red and black color, respectively.

## Taxonomy

Family: EUSCORPIIDAE Laurie, 1896

Subfamily: EUSCORPIINAE Laurie, 1896

Genus: *Euscorpius* Thorell, 1876

Subgenus: *incertae sedis*

*Euscorpius borovaglavaensis flavus* n. ssp. Vignoli

(Figs. 5–7, 11-19, 20, 22-23, Tab. 3)

ZooBank registration: urn:lsid:zoobank.org:act:DC988BBD-A9A6-4F3A-BC51-68D5E746AF20

TYPE MATERIAL. Croatia: Dinaric Alps:

**Holotype:** adult ♂ (CNHM789), **Simurđići**, Bruvno - Klapavica, Lika, 44°25'23"N, 15°52'22"E, 730 m a.s.l., 14.IX.2022, leg. M. Vuković.

**Paratypes:** 1 adult ♀ (MSNTSC700), **Simurđići**, Bruvno - Klapavica, Lika, 44°25'23"N, 15°52'22"E, 730 m a.s.l., 25.IV.2022, N. Tvrtković leg.; 1 adult ♀ (CNHM790), **Trnavac**, Church ruins, Grahovci, Mt. Mala Kapela, Lika, 44°44'54"N, 15°33'48"E, 720 m a.s.l., 28.IX.2020, N. Tvrtković leg.; 1 adult ♀ (CNHM791), **Kik**, St. Petka Church, Lovinac-Gornja Ploča, Ličko polje, Lika, 44°25'32"N, 15°38'28"E, 603 m a.s.l., 17.X.2020, N. Tvrtković leg.; 1 adult ♀ (CNHM792), **Ondić**, Lika, 44°28'35"N, 15°46'38"E, 735 m a.s.l., 07.IV.2021., M. Vuković leg.; 1 adult ♂ (MNSB14017), **Mogorić - Medak**, Ličko polje, Lika, 44°28'51"N, 15°33'45"E, 590 m a.s.l., 05.X.2018, F. Rebrina leg.; 1 adult ♂ (NHMW29981), **Bjelobabe**, Zir Hill, Ličko polje, Lika, 44°26'26"N, 15°35'54"E, 600 m a.s.l., 05.X.2018, F. Rebrina leg.

**Table 3.** Measurements (mm) and pectine tooth count of type specimens of *Euscorpius borovaglavaensis flavus* n. ssp.<sup>1</sup> CarA = Distance from center of median eyes to anterior carapace margin.<sup>2</sup> CarP = Distance from center of median eyes to posterior carapace margin.<sup>3</sup> Chela width = Wchel-A (TROPEA *et al.*, 2014).<sup>4</sup> car+mes+met = carapace + mesosoma + metasoma. In pedipalp total trochanter length is not included.

|                |                             | Holotype ♂  |               | Paratypes ♀ |             |             | Paratypes ♂     |               |
|----------------|-----------------------------|-------------|---------------|-------------|-------------|-------------|-----------------|---------------|
|                |                             | CNHM<br>789 | MSNT<br>SC700 | CNHM<br>790 | CNHM<br>791 | CNHM<br>792 | MCSNBG<br>14017 | NHMW<br>29981 |
| Carapace       | anterior width              | 2.1         | 2             | 1.9         | 2           | 2.1         | 1.7             | 2.1           |
|                | posterior width             | 5.6         | 5.2           | 4.8         | 5.6         | 5.3         | 4.5             | 5.4           |
|                | length                      | 5.6         | 5.2           | 4.7         | 5.2         | 5.1         | 4.5             | 5.5           |
|                | CarA <sup>1</sup>           | 2.6         | 2.4           | 2.1         | 2.3         | 2.3         | 1.9             | 2.5           |
|                | CarP <sup>2</sup>           | 3           | 2.8           | 2.6         | 2.9         | 2.8         | 2.6             | 3             |
| Chela          | width <sup>3</sup>          | 3.9         | 3.6           | 3.1         | 3.6         | 3.5         | 2.9             | 3.8           |
|                | length                      | 9.7         | 9.1           | 8           | 9.4         | 8.9         | 7.6             | 9.3           |
|                | length of<br>movable finger | 6           | 5.2           | 4.6         | 5.6         | 5           | 4.5             | 5.8           |
|                | length of manus             | 5.1         | 4.6           | 4.1         | 4.7         | 4.4         | 4               | 4.9           |
| Patella        | width                       | 1.9         | 1.7           | 1.5         | 1.9         | 1.7         | 1.4             | 1.8           |
|                | length                      | 4.6         | 4.3           | 3.9         | 4.3         | 4.1         | 3.7             | 4.5           |
| Femur          | width                       | 1.7         | 1.7           | 1.4         | 1.2         | 1.5         | 1.4             | 1.6           |
|                | length                      | 4.5         | 4.2           | 3.8         | 4.4         | 3.9         | 3.7             | 4.5           |
| Pedipalp       | total length                | 23.9        | 22.2          | 19.8        | 22.8        | 21.3        | 19              | 23.2          |
| Tergite I      | length                      | 0.6         | 0.6           | 0.7         | 0.8         | 0.6         | 0.6             | 0.5           |
| Tergite II     | length                      | 1           | 1.2           | 0.9         | 1.2         | 1           | 0.9             | 1.1           |
| Tergite III    | length                      | 1.4         | 1.7           | 1.2         | 1.9         | 1.7         | 1.4             | 1.7           |
| Tergite IV     | length                      | 1.8         | 2             | 1.3         | 2.3         | 2.1         | 1.7             | 2.1           |
| Tergite V      | length                      | 1.9         | 1.9           | 1.6         | 2.5         | 2.4         | 1.9             | 2.3           |
| Tergite VI     | length                      | 2.2         | 2             | 1.6         | 2.6         | 2.4         | 2               | 2.4           |
| Tergite VII    | length                      | 2.7         | 2.3           | 1.8         | 3.1         | 2.9         | 2.5             | 3             |
| Mesosoma       | total length                | 11.6        | 11.7          | 9.1         | 14.4        | 13.1        | 11              | 13.1          |
| Metasoma I     | width                       | 2           | 1.9           | 1.7         | 1.9         | 1.7         | 1.6             | 1.9           |
|                | length                      | 2.1         | 1.9           | 1.6         | 1.8         | 1.7         | 1.6             | 2.1           |
| Metasoma II    | width                       | 1.8         | 1.7           | 1.5         | 1.6         | 1.6         | 1.4             | 1.7           |
|                | length                      | 2.5         | 2.2           | 1.9         | 2.3         | 2           | 1.9             | 2.6           |
| Metasoma III   | width                       | 1.7         | 1.6           | 1.4         | 1.5         | 1.5         | 1.3             | 1.6           |
|                | length                      | 2.8         | 2.5           | 2.2         | 2.5         | 2.3         | 2.1             | 2.9           |
| Metasoma IV    | width                       | 1.6         | 1.5           | 1.4         | 1.5         | 1.4         | 1.3             | 1.5           |
|                | length                      | 3.5         | 3             | 2.6         | 3.2         | 2.8         | 2.6             | 3.5           |
| Metasoma V     | width                       | 1.5         | 1.4           | 1.3         | 1.4         | 1.4         | 1.2             | 1.4           |
|                | length                      | 5.6         | 4.7           | 4.2         | 4.7         | 4.4         | 4.3             | 5.6           |
| Metasoma I-V   | length                      | 16.5        | 14.3          | 12.5        | 14.5        | 13.2        | 12.5            | 16.7          |
| Vesicle        | width                       | 1.8         | 1.5           | 1.4         | 1.4         | 1.4         | 1.6             | 1.8           |
|                | length                      | 4.5         | 3.2           | 2.6         | 3           | 3           | 3.5             | 4.3           |
|                | height                      | 2.4         | 1.5           | 1.3         | 1.4         | 1.4         | 1.9             | 2.4           |
| Aculeus        | length                      | 1.2         | 1.2           | 1.4         | 1.4         | 1.2         | 1               | 1.3           |
| Telson         | length                      | 5.7         | 4.4           | 4           | 4.4         | 4.2         | 4.5             | 5.6           |
| Metasoma       | length                      | 22.2        | 18.7          | 16.5        | 18.9        | 17.4        | 17              | 22.3          |
| Total length   | car+mes+met <sup>4</sup>    | 39.4        | 35.6          | 30.3        | 38.5        | 35.6        | 32.5            | 40.9          |
| Pectines teeth | L/R                         | 9/9         | 8/8           | 7/7         | 8/8         | 7/8         | 9/9             | 8/9           |



Plate 1, Figs. 5-10.

Figs. 5-7. *Euscorpium borovaglavaensis flavus* n. ssp.:

Fig. 5. Dorsal habitus, adult ♂, holotype (CNHM789), scale: 5.6 mm.

Fig. 6. Ventral habitus, adult ♂, holotype (CNHM789), scale: 5.6 mm.

Fig. 7. Dorsal habitus, adult ♀, paratype (CNHM791), scale: 5.2 mm.

Figs. 8-10. *Euscorpium borovaglavaensis borovaglavaensis* Tropea, 2015:

Fig. 8. Dorsal habitus, adult ♂ (ZMBH76), scale: 6 mm.

Fig. 9. Ventral habitus, adult ♂ (ZMBH76), scale: 6 mm.

Fig. 10. Dorsal habitus, adult ♀ (CNHM787): scale: 5.4 mm.

#### ADDITIONAL MATERIAL.

1 adult ♂ (VVZC1374), 3 adults ♀♀, **Simurđići**, Bruvno-Klapavica, Lika, 44°25'23"N, 15°52'22"E, 730 m a.s.l., leg. A. Lemić, M. Vuković; 25.IV.2021 (NHMW29982, CNHM793), 14.IX.2022 (VVZC1378), M. Vuković leg.; 2 adults ♀♀ (ZMBH77, VVZC1376), **Ondić**, Lika, 44°28'35"N, 15°46'38"E, 753 m a.s.l., 7.VII.2021, N. Tvrtković leg.; 1 adult ♂ (VVZC1377), **Bjelobabe**, Zir Hill, Ličko polje, Lika, 44°26'26"N, 15°35'54"E, 600 m a.s.l., 05.X.2018, F. Rebrina, N. Tvrtković leg.; 1 adult ♀ (CNHM795), **Mala Plana**, Gornje Pazarište, Mt. Velebit, 44°39'06"N, 15°09'36"E, 700 m a.s.l., 25. IV.2021, N. Tvrtković, M. Vuković, A. Lemić leg.; 1 subadult ♀ (PMST11), **Vojvodići**, Mazin, Lika, 44°26'52"N, 15°57'02"E, 807 m a.s.l., 15.VIII.2020, M. Vuković, A. Lemić leg.; 1 adult ♀ (CNHM796), **Prpino brdo**, Mazin, Lička Plješevica Mt., Lika, 44°28'31"N, 15°58'35"E, 940 m a.s.l., 29.IX.2022, M. Vuković leg.; 1 adult ♀ (CNHM794) **Krasno**, Polje, Mt. Velebit, Lika, 44°49'03"N, 15°04'02"E, 750 m a.s.l., 20.VI.2022, Š. Tomaić leg.; 1 adult ♂ + 2 juv. (NHMW2162), **Šolta Island**, Dalmatien, 11.9.1929, leg. F. Werner, det. as *Euscorpium carpathicus mesotrichus* Hadži, 1929.



**Plate 2, Figs. 11-13.**

*Euscorpium borovaglavaensis flavus* n. ssp.:

**Fig. 11.** Carapace dorsal aspect, adult ♂, holotype (CNHM789), scale 2.6 mm.

**Fig. 12.** Dorsal retrolateral aspect of pedipalp chela, adult ♂, holotype (CNHM789), scale: 2.5 mm.

**Fig. 13.** Dorsal retrolateral aspect of pedipalp chela, adult ♀, paratype (CNHM791), scale: 2.2 mm.

**ETYMOLOGY.** Taxon name refers to the body orange brown to yellowish (*"flavus"* in Latin) color, in contrast to the genetically closest relative, in combination with the genus name masculine in gender.

**DIAGNOSIS.** Medium-large taxon with adults reaching 40.9 mm in total length. Overall coloration is light orange brown or light sand yellow with yellow chelicera, legs and telson. Pedipalp chela finger margins type A. Pedipalp patellar external trichobothria: *eb*: 4, *eb<sub>a</sub>*: 4, *esb*: 2, *em*: 4, *est*: 4, *et*: 7; ventral aspect with 10 (9-11) trichobothria. Number of pectinal teeth: ♂=9, ♀=8. Presence of metasoma ventral median carina on segment IV. Marked metasoma ventral median carina and intercarinal surface granulation on segment V. All sternites of the same color, marbling absent or very light only on metasomal segments and chelicera.

**DESCRIPTION.** This description is based on holotype adult ♂ (CNHM789, Figs. 5, 6, 11, 12, 14-20, 22) and paratype adult ♀ (CNHM791, Figs. 7, 13, 23). Morphometrics are provided in Tab. 3.

**Color** (Figs. 5-7). Carapace, cheliceral teeth, tergites, sternites (♂), metasoma, pedipalp femur and chela manus, distal portions of leg ungues and dactyl orange brown (NCS S 6030-Y30R) with darker pedipalp chela fingers and telson aculeus (NCS S 8010-Y50R). Pedipalp patella is lighter than femur and chela, light brown beige (NCS S 3050-Y10R). Pedipalp chela finger denticle rows black brown (NCS S 8505-Y20R). Chelicera tibia, carapace (♀), tergites (♀), legs, genital operculum, sternites (♀) and

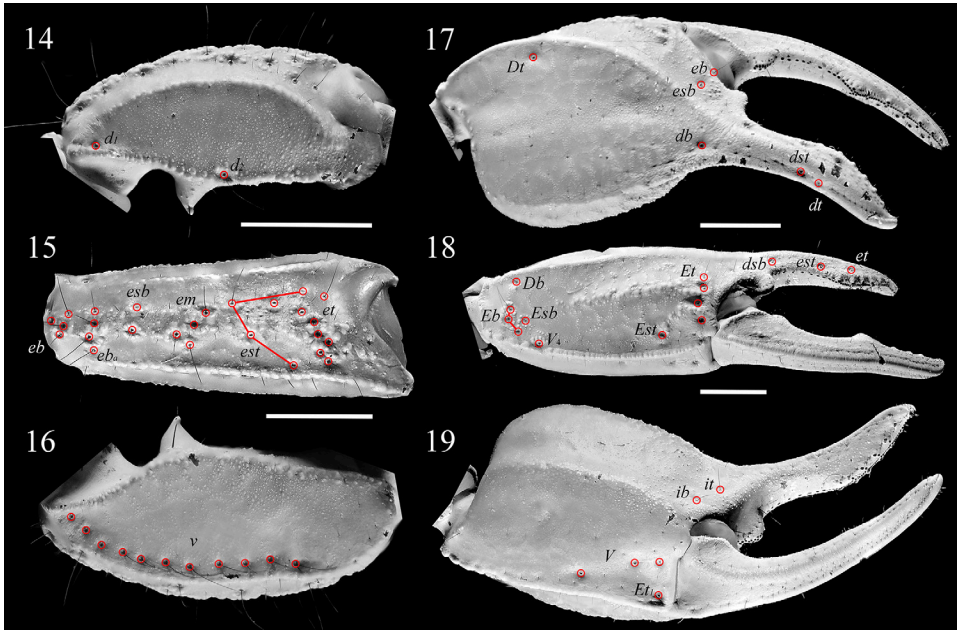


**Plate 3, Figs. 14-19.**

*Euscorpius borovaglavaensis flavus* n. ssp., adult ♂, holotype (CNHM789):

**Fig. 14.** Patella dorsal aspect, scale: 1.9 mm.

**Fig. 15.** Patella retrolateral aspect, scale: 1.4 mm.

**Fig. 16.** Patella ventral aspect, scale as for Fig. 15.

**Fig. 17.** Dorsal aspect of pedipalp chela, scale: 1.6 mm.

**Fig. 18.** Retrolateral aspect of pedipalp chela, scale: 1.4 mm.

**Fig. 19.** Ventral aspect of pedipalp chela, scale as for Fig. 18.

pectines light sand yellow (NCS S 2020-Y10R) but telson vesicle slightly darker sand yellow (NCS S 3040-Y10R). Leg granules from orange brown (NCS S 6030-Y30R) to light sand yellow (NCS S 2020-Y10R), while granules and carinae can vary from orange brown (NCS S 6030-Y30R) on metasoma to black brown (NCS S 8505-Y20R) on pedipalps. Plural and intersegmental (tergites and sternites) membranes are grey (NCS S 7502-G).

*Chelicerae.* Manus dorsal surface slightly marbled on distal portion, smooth with one macroseta and several microsetae on distal margin; ventral surface with brush-like setae on entire prolateral margin. Movable finger with ventral distal denticle longer than dorsal distal denticle; dorsal aspect with two small subdistal denticles, one larger medial denticle and one basal denticle, smallest of the series; scattered microsetae. Ventral edge without denticles and covered with brush-like setae on 2/3 of finger length. Serrula absent. Fixed finger with four denticles; basal and medial very close forming a bicuspid and covered with brush-like setae like the movable finger, no visible microsetae.

*Carapace* (Fig. 11). As long as wide, acarinate, with anterior margin straight with small granules (smaller in ♀); posterior margin slightly convex, smooth except later-

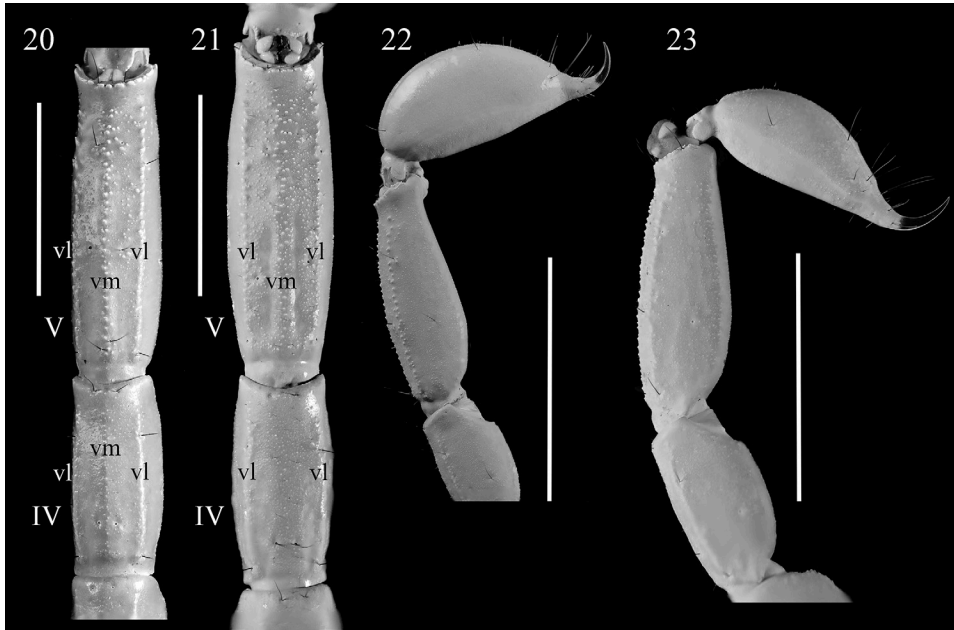


**Plate 4, Figs. 20-23.**

*Euscorpium borovaglavaensis flavus* n. ssp.:

**Fig. 20.** Ventral aspect of metasoma segments IV-V, adult ♂ holotype (CNHM789), scale: 3.3 mm.

**Fig. 22.** Lateral aspect of metasoma segment V and telson, adult ♂ holotype (CNHM789), scale: 4.4 mm.

**Fig. 23.** Lateral aspect of metasoma segment V and telson, adult ♀, paratype (CNHM791), scale: 5.7 mm.

*Euscorpium borovaglavaensis borovaglavaensis* Tropea, 2015: adult ♂ (ZMBH76):

**Fig. 21.** Ventral aspect of metasoma segments IV-V, scale: 3.6 mm.

**Abbreviations:** IV: metasoma segment IV; V: metasoma segment V; vl: ventral lateral carinae; vm: ventral median.

ally where small granules are present. Marbling absent. Anterior margin with four large macrosetae; two behind median ocelli and two on median lateral areas. Anterior, anterior lateral and posterior margins with scattered microsetae. Lateral margins with small crenulate granules. Entire surface finely granulated except for anterior lateral portions behind lateral ocelli; larger granules are present on lateral areas close to posterior lateral furrows. Anterior median sulcus evident but not as deep as posterior median sulcus; posterior lateral and posterior marginal sulci evident but shallow. Lateral ocelli pattern Type 2A with mediolateral major (MLMa) ocelli larger than posterolateral major (PLMa) ocelli. Median ocular tubercle averagely developed with two median ocelli situated in anterior half of carapace.

*Pedipalps. Coxa and trochanter.* Pedipalp coxa granulate with larger and darker crenulate granules on dorsal retrolateral margin and ventral prolateral margins. Macrosetae and microsetae on dorsal and ventral surfaces but more on the latter surface. Trochanter with darker distinct crenulate granules on dorsal, ventral (smaller) and prolateral surfaces; macrosetae and microsetae on prolateral surface. In ♀ the granulation is weaker except for coxa which is similar. *Femur.* As long as patella. Dorsal prolateral carinae tuberculated with tubercles forming a continuous black brown row; dorsal

retrolateral carinae with tubercles similarly sized as for pro lateral carinae but not forming a continuous row, every granule is separate and with the tips inclined towards distal margin. Retrolateral median carinae shorter than dorsal retrolateral carinae with tubercles size like the dorsal retrolateral carinae but more spaced. Retrolateral ventral carinae vestigial with few tubercles on proximal portion. Ventral pro lateral carinae with largest tubercles and straight tips. Pro lateral median carinae close to pro lateral ventral carinae and composed by a few scattered tubercles ( $\sigma=10-14$ ,  $\text{♀}=10-12$ ) of different sizes, some as large as those for ventral pro lateral carinae. All intercarinal surfaces finely granulated with larger scattered granules on dorsal and ventral surfaces. Microsetae on all surfaces and macrosetae on pro lateral and retrolateral surfaces. In  $\text{♀}$  all the same as for  $\sigma$  but with slightly less developed granulation. *Patella* (Figs. 14-16). Dorsal pro lateral carinae weak comprising granules increasing in size from proximal to distal portion and forming a continuous, or almost continuous, row. Dorsal retrolateral carinae smooth, shiny with tubercles barely visible. Retrolateral median carinae granulated with several smooth accessory tubercles. Ventral retrolateral carinae like dorsal retrolateral carinae but with granules tips more distinguishable. Ventral pro lateral carinae with distinct rounded tubercles, larger from mid to apical portion. Dorsal intercarinal surface finely granulated, slightly larger (less than femur), on distal portion. Retrolateral intercarinal surface smooth with sparse granules, ventral intercarinal as for dorsal intercarinal surface with larger granules on pro lateral portion; pro lateral intercarinal surface smooth on proximal area and finely granulated from mid to distal area. Microsetae on all surfaces and two macrosetae on pro lateral surface, one on moderately developed dorsal patellar spur. In  $\text{♀}$  all the same as for male except for the granule dimensions which are reduced. *Chela* (Figs. 12, 13, 17-19). Stocky appearance, 2.5-2.6 times longer than wide. Manus with dorsal pro lateral carinae smooth and few distinct granules on proximal end portion. Dorsal retrolateral carinae strong, smooth with one separated tubercle on proximal distal end. Ventral retrolateral carinae similar as dorsal retrolateral carinae but with 4-5 distinct tubercles (less marked in  $\text{♀}$ ). Ventral pro lateral carinae formed by small granules. Retrolateral median carinae with tubercles decreasing in size from distal to proximal margin. Dorsal and ventral intercarinal finely granulated with few tubercles on proximal margin. Retrolateral intercarinal with sparse small granules and tubercles close to all trichobothria. Pro lateral intercarinal surface finely granulated with sparse slightly larger spiny granules; dorsal and ventral areas, close to carinae with spiny granules increasing in size. Marmoration macrosculpture and microsetae on all surfaces. Macrosetae on all surfaces except on retrolateral surface. Finger margins strongly undulate in  $\sigma$  (Type A) and undulate in  $\text{♀}$ . Movable finger ( $\sigma$ ) with proximal lobe similar in size to medial lobe and long proximal notch; both lobes with very close dark rounded tubercles and spaced short elongated denticles on the notch. Distal portion with distal denticle and median denticle row with distinct small tubercles; five (R) and four (L) retrolateral denticles and six pro lateral denticles together with four inner accessory denticles. Proximal and medial lobe are similar in size in  $\text{♀}$  while the proximal notch is shallow but distinguishable; tubercles on notches are less imbricated than on  $\sigma$  and, except for proximal notch, where the denticles are slightly larger, all other denticles are similar in size with seven retrolateral and six pro lateral denticles and four inner accessory denticles. Fixed finger of  $\sigma$  with large proximal lobe and deep proximal notch ending with a moderate medial lobe; similar dentition on lobe and notch as on movable finger. Apical portion curved towards movable finger with distal denticle and median denticle row similar to that of movable

finger but with five retrolateral and six (L)-five (R) prolateral denticles with four inner accessory denticles. Proximal lobe in ♀ with dimensions like movable finger proximal lobe; similar dentition as on movable finger and with six retrolateral, six prolateral and four inner accessory denticles. Trichobothria pattern neobothriotaxic Type C. Femur with three trichobothria: *d*, *e* and *i*; with *d* at the same distance from *i* and *e*. Patella (♂) with a total of 40 trichobothria: two dorsal:  $d_1$ - $d_2$  and one internal: *i* close to dorsal prolateral carinae; eleven ventral; twenty-six external: *eb* (4),  $eb_a$  (4), *esb* (2), *em* (4), *est* (4), *et* (8). Paratype (♀) patella as for holotype except for ventral (left 10/right 11) and external *et* (7/7) trichobothria series. Chela with 26 trichobothria; manus with two dorsal: *Dt*, *db*; fifteen external: *Eb* (3), *Esb*,  $V_d$ , *Db*, *Est*, *Et* (4), *eb*, *esb*; two internal: *ib*, *it*; four ventral: *V* (3), *Et*. Fixed finger with five trichobothria: two dorsal: *dst*, *dt*; and three external: *dsb*, *est*, *et*.

**Sternum.** Coxosternal region smooth with few sparse setae on coxapophysis and coxae of legs. Sternum pentagonal shape, Type 2. Length approximately equal to posterior width; smooth with 3 macrosetae on lateral lobes. Posterior emargination deep.

**Genital operculum.** Partially divided longitudinally; smooth, shiny with two macrosetae and a few fine sparse setae. Genital papillae externally visible for ♂.

**Pectines.** Basal piece with four macrosetae and few microsetae. Marginal lamellae comprising three sclerites with several microsetae. Middle lamellae with five sclerites, proximal sclerites are fused, fewer setae than on marginal lamellae. Fulcra with 8 (♂) and 7 (♀) sclerites with few setae. Teeth number, 9-9 (♂) and 8-8 (♀); first distal teeth with more setae than on other teeth.

**Mesosoma.** All tergites acarinate, surfaces I-VII, finely shagreened with posterior median surfaces smooth, shiny; surface VII with coarse larger granules on lateral posterior margins. Sparse macrosetae on all tergites, especially on tergite posterior margins. Sternites, surfaces III-VII punctuated, smooth and shiny with small and elongated spiracles. Sparse macrosetae on all sternites more concentrated on lateral and posterior margins.

**Legs.** Coxae of legs I-IV ventrally smooth, coxae I-II with reddish tubercles on prolateral margin but coxae III-IV with small reddish tubercles. Dorsal surface of all coxae with reddish tubercles, larger on coxa IV. Trochanters of legs I-IV with sparse pale small tubercles on dorsal and prolateral surfaces; ventral surfaces smooth for legs II-IV and with sparse pale tubercles on leg I. Femurs of all legs with reddish tubercles forming a dorsal carina on entire segment length. Femur of legs II-III with additional row of tubercles on dorsal prolateral margin. Ventral surface of femur with two distinct carinae, prolateral and retrolateral, with reddish crenulated tubercles; smaller and paler on leg IV. Intercarinal surfaces weakly and finely granulated, especially on prolateral aspect. Femur carination similar for ♀ but with smaller and paler tubercles. Patella of all legs with dorsal and lateral portions smooth and with reddish tubercles on ventral surface from mid to distal portion, crenulate on legs I-III and rounded, smaller on leg IV for ♂ (for leg I paratype MCSNBG-14017 has been examined since missing on holotype). For ♀ all tubercles are weaker and paler and on leg IV the granulation is almost absent, showing few small tubercles on distal portion only. Tibial spur absent and two pedal spurs on all legs. Basitarsus I/II with retrolateral ventral stout spinules (leg I (L/R): ♂ MCSNBG-14017=7/10, ♀=10/12; leg II (L/R): ♂ MCSNBG-14017=7/9, ♀=8/8). Tarsus I-IV with a row of ventral median spinules and one pair of distal spinules (leg III (L/R): ♂=10/10; ♀: missing/10). Sparse microsetae and mac-

rosetae on all segments, more on basitarsus and tarsus. Ungues and dactyl as for genus. All segments are same in color, marbling absent.

*Metasoma and telson* (Figs. 20, 22, 23). Ventral median carina absent on segment I-II, vestigial on segment III, weak and smooth with very small granules on segment IV and moderately developed, crenulated, on segment V with tubercles more spread on lateral distal portion. Ventral lateral carina obsolete on segment I, vestigial on segment II-III, weak on segment IV with few granules on distal portion, and crenulated on segment V with tubercles increasing in size from proximal to distal portion. Lateral median carinae vestigial on segments I-IV and absent on segment V; weaker on all segments for ♀. Dorsal lateral carinae weak on segment I and composed of small sparse granules larger on proximal portion; similar on segments II-IV but with larger and darker granules on distal portion. Segment V dorsal lateral carinae rounded with several very small crenulated sparse tubercles. Dorsal and lateral intercarinal surfaces of all segments finely shagreened. Ventral intercarinal surfaces smooth, punctuated on segments I-II; slightly shagreened on segments III-IV, scattered small/medium size granules from basal 2/5 to distal portion on segment V. Macrosetae on lateral and ventral surfaces of all segments. Anal arch carina with small tubercles. Carination and granulation in ♀ as for ♂. Weak marbling on segments II-V increasing intensity from proximal to distal segments on ♀, absent on all segments on ♂. Telson vesicle swollen in ♂ (almost 60% higher than for ♀) and elongated, as high as wide and as long as twice the height in ♀. Dorsal proximal portion slightly concave. All surfaces are homogeneously finely granulated. Marbling absent in ♂ while present in ♀ showing two well defined lighter stripes on ventral surface and one lighter stripe from proximal to distal margin of lateral surfaces. Sparse macrosetae and microsetae between distal vesicle margin and proximal aculeus margin. Aculeus more curved and lighter in color at proximal margin while dark at distal margin in ♂; less curved and homogeneous in color in ♀.

## Variability

In the total of 19 examined specimens, 17 adults (6 ♂♂, 11 ♀♀) and 2 subadults (♀♀), some intraspecific variability has been observed. Some color variability has been observed only in color intensity with lighter and darker specimens from yellowish to orange brown. Even if all the specimens examined show marbling on metasomal segments, in some specimens (5/19) they show an evident darkening on segments IV-V due to marbling. Trichobothria variability as following: patella ventral counts: 9-8 (5% (1/19)), 9-9 (10% (2/19)), 7-10 (5% (1/19)), 11-9 (5% (1/19)), **10-10** (42% (8/19)), 10-11 (5% (1/19)), 11-11 (21% (4/19)), 12-12 (5% (1/19)); patella external counts: *eb*= 4-3 (5% (1/17)); *eb<sub>a</sub>*= 3-4 (5% (1/17)) *em*= 0/4 (5% (1/17)), 4/3 (11% (2/17)); *est*= 5/4 (5% (1/17)), *et*= 7/8 (11% (2/17)), 7/7 (58% (10/17)), 8/8 (29% (5/17)). The following pectinal teeth variation have been observed, ♀♀= 7/7 (1/13), 7/8 (4/13), **8/8** (5/13), 9-8 (1/13), 9/9 (1/14); ♂♂= 8/8 (1/6), 8/9 (1/6), **9/9** (4/6).

We also found variability of pedipalp chela finger denticle count; on some specimens the denticles are clearly separated while for some specimens, especially next to the medial lobe, the denticles are very close and difficult to recognize. We counted only the denticles that are clearly distinguishable resulting in the following variability: movable finger: retrolateral denticles (L/R): 4-7 (mostly 6), prolateral denticles (L/R): 5-6 (mostly 6), accessory denticles (L/R): 4-6 (mostly 4). Fixed finger: retrolateral denticles

(L/R): 4-6 (mostly 6), prolateral denticles (L/R): 4-6 (mostly 6), accessory denticles (L/R): 1-4 (mostly 3). Although a more common number of spinules on leg tarsus and basitarsus is evident we have seen some variability: ventral median spinules on tarsus leg III (L/R): 7-14 (mostly 11), retrolateral ventral spinules on basitarsus leg I (L/R): 3-17 (mostly 8), basitarsus leg II (L/R): 2-9 (mostly 8).

Lateral ocelli have been observed under UV light to detect also the minor ocelli and only one individual (NHMW29981) bears a third small ocellus (ADMi) on one side (R) of the carapace showing a Type 3B pattern, while all other specimens have Type 2A.

An interesting finding was that two specimens had abnormal legs. One sub adult ♀ (CNHM790) with a completely missing basitarsus and a reduced tarsus on left leg I and a second specimen, adult ♂ (NHMW29981), with a completely missing tarsus on the right leg II, both with complete but very small unguis and dactyl. Although it is not possible to know the reason for the malformation, it is very similar to that described by WATZ & DUNLOP (2022) and therefore we probably found two cases of incomplete regeneration. The fact that 11% percent of our analyzed samples show regeneration could be a coincidence, or a not uncommon phenomenon in euscorpids, however in our opinion worthy of note.

### Differences from nominal subspecies

*Euscorpius borovaglavaensis flavus* n. ssp. can be distinguished from *Euscorpius borovaglavaensis borovaglavaensis* Tropea, 2015 in (1) metasoma ventral median carina of segment IV: it is in *E. b. flavus* n. ssp. always present (Fig. 20), both in adult ♀♀ and ♂♂ and in subadults, while it is absent in *E. b. borovaglavaensis* (Fig. 21), and (2) metasoma ventral median carina of segment V in *E. b. flavus* n. ssp. is strong, more marked with larger distinct crenulated tubercles (Fig. 20) than for nominal subspecies where the tubercles are smaller and closer together forming a broader, less distinct ventral median carina (Fig. 21). In addition (3), the ventral intercarinal surface is less granulated than for nominal subspecies where several small granules are present on entire segment length (Fig. 21), and (4) sternite VII has same color as sternites III-VI (Fig. 6), while nominal subspecies has sternite VII darker and similar in color as metasoma segments (Fig. 9) – it is the most remarkable trait of overall body color differences - in *E. b. flavus* n. ssp. light orange to yellowish sand (Figs. 5-7), while nominal subspecies is dark brown (Figs. 8-10), in (5) chelicera manus dorsal marbling in *E. b. flavus* n. ssp. slightly on distal portion, while for nominal subspecies the marbling is strong and covering entire dorsal manus, in (6) telson marbling in *E. b. flavus* n. ssp. absent or weak, while in nominal subspecies present strong.

### Differences from other, similar *Euscorpius* species

*Euscorpius borovaglavaensis* Tropea, 2015 can be distinguished from *Euscorpius tergestinus* (C. L. Koch, 1837) from Eastern Adriatic coastal (not island) populations, in (1) metasoma segment IV ventral median carina development, in *E. tergestinus* obsolete, but present or absent in *E. borovaglavaensis*, difference in ventral intercarinal surface of metasomal segment, in (2) by metasomal segment V, in *E. tergestinus* it is mostly smooth or with few small granules, while it is present and more granulated in *E. borovaglavaensis*, and by (3) different body color, in *E. tergestinus* reddish, reddish brown or brown – in *E. borovaglavaensis* extremely variable, different in subspecies, but never similar to that of *E. tergestinus*.

*Euscorpius borovaglavaensis flavus* **n. ssp.** can be distinguished from *Euscorpius tergestinus* (C. L. Koch, 1837) from coastal Eastern Adriatic populations in (1) metasoma segment IV: in *E. tergestinus* obsolete ventral median carina, in *E. b. flavus* **n. ssp.** it is always present; by (2) the metasoma segment V: ventral intercarinal surface in *E. tergestinus* it is mostly smooth or with small scattered granules, while *E. b. flavus* **n. ssp.** bears several small-medium granules, and (3) by different body color. Nominal subspecies can be distinguished from *E. tergestinus* in (1) different whole body color and marbling (TROPEA, 2015), but especially in color of sternite VII, which is in *E. tergestinus* always the same as in other sternites, in *E. b. borovaglavaensis* noticeably darker than color of other sternites, but the same as the color in metasoma segments, and (2) in metasoma segment IV *E. tergestinus* has obsolete ventral median carina, in *E. b. borovaglavaensis* ventral median carina is absent.

Among other *Euscorpius* species with similar trichobothria and pectinal teeth counts the new subspecies can be distinguished as follows: *E. feti* Tropea, 2013, has a slender morphology supported by morphometrics and only one distal spinule in ventral median row on tarsus (TROPEA, 2013b); *E. corcyraeus* Tropea & Rossi, 2012 has pedipalp fingers Type C, a considerably swollen telson vesicle in males and is a small species reaching a maximum total length of 23 mm (TROPEA & ROSSI, 2012); *E. vailatii* Tropea & Fet, 2015 has metasoma ventral median carinae absent or obsolete on segment IV, larger pedipalp chela width in males than in females, smaller in total length, maximum 34.5 mm (TROPEA & FET, 2015); *E. candiota* Birula, 1903 is characterized by having smooth to obsolete metasomal carination on segments II-IV (FET *et al.*, 2013) and less marked ventral lateral and ventral median carinae on segment V; *E. balearicus* Di Caporiacco, 1950 has a reduced metasoma with carination almost absent (GANTENBEIN *et al.*, 2001).

## Distribution

Known only in Croatia. After our present data, Western part of Middle Dalmatia (Šolta Island, Mt. Svilaja, southern slopes of Mt. Troglav, Mt. Dinara) and the Lika karstic plateau between the mountains Velebit, Velika Kapela, Mala Kapela and the southwestern slopes of the Lička Plješevica Mts. (Fig. 1). Vertical range probably from sea level to cca. 1200 m a.s.l., like nominal subspecies, too. After our really incomplete samples in Croatia nominal subspecies inhabited eastern part of Middle Dalmatia (Split?, Dubrava E Split, Mt. Biokovo, Mt. Kamešnica) and in southern Bosnia and Herzegovina all open karst habitats with Mediterranean influence, probably to cca. 1200 - 1300 m a.s.l. including the northern slopes of Troglav and Dinara. On Dinara, reached from the northern side one high mountain valley (Duler, 1200 m a.s.l., Croatia, just near the state border). Distribution border in southern Bosnia and Herzegovina is currently unknown even if isolated, probably introduced samples, are known more northern in Barevo (TROPEA, 2015) and in Niš, Serbia (PODNAR *et al.*, 2021).

## Ecology: habitats and sympatric scorpions

Habitats of *E. b. flavus n. ssp.* are almost dry rocky pastures, sometimes with sink-holes, dry rocky heath with bracken (*Pteridium aquilinum*) or rarely with common heather (*Calluna vulgaris*), rocky scrubland or garrigues, dry stone walls (stone fences), piles, abandoned quarries, rocky roadsides, all in two climazonal Mediterranean belts. In (1) the lower more thermophilic coastal belt of manna ash (*Fraxinus ornus*) with evergreen holm oak (*Quercus ilex*) forests or pubescent oak (*Quercus pubescens*) with oriental hornbeam (*Carpinus orientalis*) forests, too. On Svilaja and in the Lika area in (2) higher sub-montane or montane forest belt with colder winters: pubescent oak (*Quercus pubescens*) with hop hornbeam (*Ostrya carpinifolia*) forests. A rough distribution of forest types can be seen in TRINAJSTIĆ & ŠUGAR (1968: Fig. 2). The highest or northern localized habitats are on western slopes with thermophilic beech forests - beech (*Fagus sylvatica*) with autumn moor grass (*Sesleria autumnalis*) or hop hornbeam (*Ostrya carpinifolia*) (VUKELIĆ, 2012).

The epigeal *Euscorpium borovaglavaensis flavus n. ssp.* in Lika region is the only scorpion species, but at higher altitudes it is parapatric with the forest species *Alpiscorpius omega* Kovařík, Štundlová, Fet & Štáhlavský, 2019 (e.g. in Krasno, on the northern slopes of Velebit Mts., above Trnavac on Mala Kapela and above Mazin on the southern slopes of Lička Plješevica). The Velebit mountain chain is the border of the coastal population of *E. tergestinus* (C. L. Koch, 1837). On Šolta Island and at lower altitudes of the western part of Middle Dalmatia between the Krka River and the Cetina River, *E. b. flavus n. ssp.* is sympatric and syntopic with *Euscorpium (Polytrichobothrius) italicus* (Herbst, 1800) (unpublished field data). In the eastern part of Middle Dalmatia the epigeal *E. borovaglavaensis borovaglavaensis* is sympatric with the cave-dweller *Euscorpium biokovensis* Tropea & Ozimec, 2020.

## DISCUSSION

The substantial intraspecific genetic distances within *Euscorpium borovaglavaensis* were previously discussed in the study by PODNAR *et al.* in 2021. Moreover, in the same paper, one of the three applied species delimitation approaches (bPTP) identified as many as four candidate species. However, the sample size in that study was extremely limited, and the phylogenetic relationships within the *E. borovaglavaensis* clade were not fully resolved. The estimated time of the initial diversification of *E. b. borovaglavaensis* and *E. b. flavus ssp. nov.*, 0.9 MYA (HPD 1.4-0.6 MYA), coincides with the period of Mid-Pleistocene Transition (MPT, 1.25 – 0.7 MYA), the Pleistocene glacial cycles shift from 41 to  $\approx$  100 KYR periodicity (CLARK *et al.*, 2006). This complex climatic change has been repeatedly shown to be an important factor impacting diversification in various animal taxa in the Mediterranean and surrounding areas (PODNAR *et al.*, 2014; SENCZUK *et al.*, 2017; GHANE-AMELEH *et al.*, 2021; PODNAR *et al.*, 2021). Those two lineages must have evolved in isolation in two separate, north-western and south-eastern, refugial areas. After the initial isolation event, the *E. b. flavus ssp. nov.* refugium located probably on the prominent hilly part of the coast between the mouth of the Krka River and Split (Western part of Middle Dalmatia) must have been further subdivided into at least three microrefugia corresponding to 3 sublineages (Fig. 2 and 3). The lack of the prominent phylogeographic structure within *E. b. borovaglavaensis* could be an artefact of insufficient sampling across the subspecies range (especially in Bosnia and Herzegovina). The present spatial distribution of haplotypes (Fig. 3) strongly indicate that

the north-western lineages spread postglacially northwards from the western side of Middle Dalmatia to the Lika karstic plateau region in the Velebit hinterland, in an area without competition from *Euscorpius (Polytrichobothrius) italicus*.

We have not found tentative contact zones between the subspecies, although we expected that they are on the southern slopes of Mt. Kamešnica and probably east of Split - around Mt. Mosor (Fig. 1). The possible cause of this is the small sample size and, particularly, insufficient sampling in border region between two subspecies. In our sample, we also did not recognize presumed hybrid specimens. The precise location of a historical finding of nominal subspecies in Split city (Fig. 1) is uncertain since the locality is marked with a question mark on the museum label. Based on morphological trait comparison, it could be assumed that the new taxon represents a good species. However, the genetic distances values (Tab. 3), although not overlapping, are lower than those typically observed between *Euscorpius* species (i. e. PARMAKELIS *et al.*, 2013; KOVAŘÍK *et al.*, 2020; PODNAR *et al.*, 2021). On the other hand, intraspecific p-distances between *E. borovaglavaensis flavus* n. ssp. and nominal subspecies (1.7 – 2.3 %) are similar to those found between the two relict cryptic allopatric scorpion species, *Alpiscorpius sigma* Kovařík, Štundlová, Fet & Šťáhlavský, 2019 and *A. omicron* Kovařík, Štundlová, Fet & Šťáhlavský, 2019 (1.5 – 2.5 %) (ŠTUNDLOVÁ *et al.*, 2019; KOVAŘÍK *et al.*, 2019; PODNAR *et al.*, 2021). The taxonomic distinction between *A. sigma* and *A. omicron* was supported only by cytogenetic traits, different diploid chromosome numbers,  $2n = 60$  versus  $2n = 58$  (ŠTUNDLOVÁ *et al.*, 2019; KOVAŘÍK *et al.*, 2019), probably since it could cause reproductive isolation between different cytotypes (“karyotype races”), in this case between relict populations. Diploid chromosome numbers vary significantly in different *Euscorpius* species (range:  $2n = 36 - 2n = 112$ ) (KOVAŘÍK & ŠTÁHLAVSKÝ, 2020), but the chromosomes of the *E. tergestinus* group have never been studied. Only a future cytogenetic approach with evidence of reproductive isolation will provide a more complete insight into the taxonomy of the whole group, including the particular case described here.

The discovery of a new epigeal allopatric cryptic taxon from the *Euscorpius tergestinus* group further west from the first described *Euscorpius borovaglavaensis* range (TROPEA, 2015), restricts the coastal distribution of *Euscorpius tergestinus* s.s. along the Eastern Adriatic from Carso Triestino to Krka River (Fig. 1) including Rab and Pag islands (PODNAR *et al.*, 2021). Our results highlight the need for the taxonomic affiliations of more easterly *E. tergestinus* s.l. populations in Croatia and Montenegro, noted in other studies: on Hvar Island (FET *et al.*, 2009), near Metković (TROPEA, 2015) and on the supralittoral of Montenegro (KARAMAN, 2020). Drawing on all the evidence, additional investigations are in progress to find, map and genetically characterize other morphologically cryptic populations belonging to “*E. tergestinus* group” on the Dinaric Alps and Eastern Adriatic coast and especially on the islands. The ongoing research is expected to shed more light on genetic and morphological intraspecific and interspecific variability and evolutionary patterns of this interesting and tricky scorpion group.

## ACKNOWLEDGEMENTS

We are indebted to Andrea Colla (Civico Museo di Storia Naturale Trieste) and Carlo Maria Legittimo (Aracnofilia – Associazione Italiana di Aracnologia), for allowing the examination of the *Euscorpius tergestinus* neotype and other useful material. We are grateful to Christoph Hörweg for the loan specimens from Naturhistorische Mu-

seum, Wien. We are grateful for help in sampling specimens in Croatia to Marijana Vuković, Ana Lemić, Štefica Tomaić, Irena Grbac, Goran Rnjak, and in Bosnia and Herzegovina to Vinko Ljubas, Tonći Rađa, Josip Skejo and Jure & Niko Kasalo. We are grateful to Paolo Magrini (Museo di Storia Naturale dell'Università di Firenze "La Specola") and Andrea Petrioli for providing contacts and relevant technical suggestions. We thank Gioele Tropea for providing publications and Gianni Pellegrini for support on the NCS - Natural Colour System<sup>®</sup> concept and application. We thank to Josip Skejo and two anonymous reviewers for their useful comments. The investigation was partially supported by Croatian Science Foundation, Grant/Award Number: HR-ZZ-IP-2016-06-9988.

Received October 15, 2023

## REFERENCES

- BOUCKAERT, R., VAUGHAN, T.G., BARIDO-SOTTANI, J., DUCHENE S., FOURMENT, M., & GAVRYUSHKINA, A., 2019: BEAST 2.5: An advanced software platform for Bayesian evolutionary analysis. *PLoS computational biology* **15**(4), e1006650
- CAIN, S., GEFFEN, E., & PRENDINI, L., 2021: Systematic revision of the Sand scorpions, genus *Buthus* Birula, 1908 (*Buthidae* C.L. Koch, 1837) of the Levant, with redescription of *Buthacus arenicola* (Simon, 1885) from Algeria and Tunisia. *Bulletin of the American Museum of Natural History*, **350**, 134 pp.
- CLARK, P.U., ARCHER, D., POLLARD, D., BLUM, J. D., RIAL, J.A., BROVKIN, V., MIX, A.C., PISIAS, N.G., & ROY, M., 2006: The Middle Pleistocene transition: Characteristics mechanisms, and implications for long-term changes in atmospheric pCO<sub>2</sub>. *Quaternary Science Reviews* **25**, 3150–3184.
- DARRIBA, D., TABOADA, G. L., DOALLO, R., POSADA, D., 2012: jModelTest 2: More models, new heuristics and parallel computing. *Nature Methods* **9**, 772. <https://doi.org/10.1038/nmeth.2109>
- DRUMMOND, A. J., RAMBAUT, A., SHAPIRO, B., & PYBUS, O. G., 2005: Bayesian coalescent inference of past population dynamics from molecular sequences. *Molecular Biology and Evolution* **22** (5), 1185–1192. <https://doi.org/10.1093/molbev/msi103>
- FET, V. & SOLEGLAD, M. E., 2002: Morphology analysis supports presence of more than one species in the "*Euscorpium carpathicus*" complex (Scorpiones: Euscorpidae). *Euscorpium* **3**, 1-51.
- FET, V., SOLEGLAD, M. E., PARMAKELIS, A., KOTSAKIOZI, P., & STATHI, I., 2013: Three more species of *Euscorpium* confirmed for Greece (Scorpiones: Euscorpidae). *Euscorpium* **165**, 1-27.
- GANTENBEIN, B., SOLEGLAD, M.E., & FET, V., 2001: *Euscorpium balearicus* Caporiacco, 1950, stat. nov. (Scorpiones: Euscorpidae): molecular (allozymes and mtDNA) and morphological evidence for an endemic Balearic Islands species. *Organisms, Diversity & Evolution* **1**, 301-320.
- GHANE-AMELEH S., KHOSRAVI M., SABERI-PIROOZ R., EBRAHIMI E., AGHBOLAGHI M. A. & AHMADZADEH F., 2021: Mid-Pleistocene transition as a trigger for diversification in the Irano-Anatolian region: evidence revealed by phylogeography and distribution pattern of the eastern three-lined lizard. *Global Ecology and Conservation* **31**, e01839. <https://doi.org/10.1016/j.gecco.2021.e01839>
- GONZÁLEZ-SANTILLIÁN, E. & PRENDINI, L., 2013: Redefinition and generic revision of the North American vaejoid scorpion subfamily Syntropinae Kraepelin, 1905, with descriptions of six new genera. *Bulletin of the American Museum of Natural History* **382**, 1-71.
- GRAHAM, M. R., WEBBER, M. M.; BLAGOEV, G.; IVANOVA, N. & FET, V., 2012: Molecular and morphological evidence supports the elevation of *Euscorpium germanus croaticus* Di Caporiacco, 1950 (Scorpiones: Euscorpidae) to *E. croaticus* stat. nov., a rare species from Croatia. *Revista Iberica de Aracnologia* **21**, 41–50.
- HALL, T. A., 1999: BioEdit: a user-friendly biological sequence alignment editor and analysis program for 15 Windows 95/98/NT. *Nucleic Acids Symposium Series* **41**, 95-98.
- HEBERT, P. D., CYWINSKA, A., BALL, S. L. & J. R. DEWAARD, 2003: Biological identifications through DNA barcodes. *Proceedings of the Royal Society, London B (Biological Sciences)* **270** (1512), 313-32.
- HJELLE, J.T., 1990: Anatomy and morphology, 9–63. In POLIS, G. A. (ed.), *Biology of scorpions*. Stanford, CA: Stanford University Press, 587 pp.

- KOVAŘÍK, F., LOWE, G., BYRONOVA, M., & ŠT'ÁHLAVSKÝ, F., 2020a: *Euscorpium thracicus* sp. n. (Scorpiones: Euscorpidae) from Bulgaria. *Euscorpium* **326**, 1-17.
- KOVAŘÍK, F. & ŠT'ÁHLAVSKÝ, F., 2020: Five new species of *Euscorpium* Thorell, 1876 (Scorpiones: Euscorpidae) from Albania, Greece, North Macedonia, and Serbia. *Euscorpium* **315**, 1-37.
- KOVAŘÍK, F., ŠTUNDLOVÁ, J., FET, V., & F. ŠT'ÁHLAVSKÝ, F., 2019: Seven new Alpine species of the genus *Alpiscorpium* Gantenbein et al., 1999, stat. n. (Scorpiones: Euscorpidae). *Euscorpium* **287**, 1-29. <https://dx.doi.org/10.18590/euscorpium.2019.vol2019.iss287.1>
- LEIGH, J., W., & BRYANT, D., 2015: Popart: full-feature software for haplotype network construction. *Methods in Ecology and Evolution* **6**, 1110-1116. <https://doi.org/10.1111/2041-210X.12410>
- LORIA, S. F. & PRENDINI L., 2014: Homology of the Lateral Eyes of Scorpiones: A Six-Ocellus Model. *PLoS ONE* **9** (12), e112913. doi:10.1371/journal.pone.0112913
- MILLER, M., PFEIFFER, W., & SCHWARTZ, T., 2010: Creating the CIPRES Science Gateway for inference of large phylogenetic trees. In Proceedings of the Gateway Computing Environments Workshop (GCE) (pp. 1-8). IEE. <https://doi.org/10.1109/GCE.2010.5676129>
- PARMAKELIS, A., P. KOTSAKIOZI, I. STATHI, S. POULIKARAKOU & V. FET, 2013: Hidden diversity of *Euscorpium* (Scorpiones: Euscorpidae) in Greece revealed by multilocus species-delimitation approaches. *Biological Journal of the Linnean Society*, London, **110**, 728-748.
- PODNDAR, M., BRUVO MAĐARIĆ, B., & MAYER, W., 2014: Non-concordant phylogeographical patterns of three widely codistributed endemic Western Balkans lacertid lizards (Reptilia, Lacertidae) shaped by specific habitat requirements and different responses to Pleistocene climatic oscillations. *Journal of Zoological Systematics and Evolutionary Research* **52** (2), 119-129. <https://doi.org/10.1111/jzs.12056>
- PODNDAR, M., GRBAC, I., TVRTKOVIĆ, N., HÖRWEG, C. & HÄRING, E., 2021: Hidden diversity, ancient divergences, and tentative Pleistocene microrefugia of European scorpions (Euscorpidae: Euscorpinae) in the eastern Adriatic region. *Journal of Zoological Systematics and Evolutionary Research* **59** (8), 1824-1849. <https://doi.org/10.1111/jzs.12562>
- RAMBAUT, A., DRUMMOND, A. J., XIE, D., BAELE, G., & SUCHARD, M. A., 2018: Posterior summarisation in Bayesian phylogenetics using Tracer 1.7. *Systematic Biology* **67**(5), 901-904. <https://doi.org/10.1093/sysbio/syy032on>
- RATNASINGHAM, S. & HEBERT, P. D. N., 2007: BOLD: The Barcode of Life Data System (<http://www.barcodinglife.org>). *Molecular Ecology Notes* **7**, 355-364.
- SENCZUK, G., COLANGELO, P., DE SIMONE, E., ALOISE, G. & CASTIGLIA, R. A., 2017: combination of long term fragmentation and glacial persistence drove the evolutionary history of the Italian wall lizard *Podarcis siculus*. *BMC Evolutionary Biology* **17**(1), 6, <https://doi.org/10.1186/s12862-016-0847-1>
- SISSOM, W. D., 1990: Systematics, biogeography and paleontology. pp. 64-160. In: POLIS, G.A. (ed), *The Biology of Scorpions*. Stanford, California: Stanford University Press, 587 pp.
- SOLEGLAD, M. E. & FET, V., 2003: The scorpion sternum: structure and phylogeny (Scorpiones: Orthosterni). *Euscorpium* **5**, 1-33. <https://dx.doi.org/10.18590/euscorpium.2003.vol2003.iss5.1>
- SOLEGLAD, M. E. & SISSOM, W.D., 2001: Phylogeny of the family Euscorpidae Laurie, 1896: a major revision. pp. 25-112. In: FET, V. & SELDEN, P. A. (eds.), *Scorpions 2001*. In Memoriam Gary A. Polis. Burnham Beeches, Bucks, UK: British Arachnological Society.
- STAHNKE, H. L. 1970: Scorpion nomenclature and mensuration. *Entomological News* **81**, 297-316.
- ŠTUNDLOVÁ, J., ŠMÍD, J., NGUYEN, P. & ŠT'ÁHLAVSKÝ, F., 2019: Cryptic diversity and dynamic chromosome evolution in Alpine scorpions (Euscorpidae: *Euscorpium*). *Molecular Phylogenetics and Evolution* **134**, 152-163. <https://doi.org/10.1016/j.ympev.2019.02.002>
- TAMURA, K., STECHER, G. & S. KUMAR, 2021: MEGA11. *Molecular Evolutionary Genetics Analysis Version 11*. *Molecular Biology and Evolution* **38** (7), 3022-3027.
- TEMPLETON, A. R., CRANDALL, K. A. & SING, C. F., 1992: A cladistics analysis of phenotypic associations with haplotypes inferred from restriction endonuclease mapping and DNA sequence data. III. Cladogram estimation. *Genetics* **132**, 619-633. DOI: 10.1093/genetics/132.2.619
- TRINAJSTIĆ, I. & ŠUGAR, I., 1968: O biljnogeografskom raščlanjenju Goransko-Ličke regije (Sur la zonation biogeographique de la region de Gorski Kotar et de Lika - in Croatian with Resume in French). *Geografski glasnik* **30**, 42-59.
- TROPEA, G., 2013a: Reconsideration of the taxonomy of *Euscorpium tergestinus* (Scorpiones: Euscorpidae). *Euscorpium* **162**, 1-23.
- TROPEA, G., 2013b: A new species of *Euscorpium* Thorell, 1876 from the western Balkans (Scorpiones: Euscorpidae). *Euscorpium* **174**, 1-10.

- TROPEA, G., 2015: A new species of *Euscorpius* Thorell, 1876 from Bosnia-Herzegovina and Croatia (Scorpiones: Euscorpiidae). *Arachnida, Rivista Arachnologica Italiana Anno I*, 5, 30-41.
- TROPEA, G. & ROSSI, A., 2012: A new species of *Euscorpius* Thorell, 1876 from Corfu, with notes of *Euscorpius* in Greece (Scorpiones, Euscorpiidae). *Ornychium* 9 (2011-2012), 27-37.
- TROPEA, G., FET, V., PARAMAKELIS, A., KOTSAKIOZI, P. & STATHI, I., 2014: Three new species of *Euscorpius* (Scorpiones: Euscorpiidae) from Greece. *Euscorpius* 190, 1-22.
- TROPEA, G. & FET, V., 2015: Two new *Euscorpius* species from central-western Greece (Scorpiones: Euscorpiidae). *Euscorpius* 199, 1-16.
- VACHON, M., 1974: Étude des caractères utilisés pour classer les familles et les genres de scorpions (Arachnides). 1. La trichobothriotaxie en arachnologie. Sigles trichobothriaux et types de trichobothriotaxie chez les scorpions. *Bulletin du Muséum National d'Histoire naturelle, Paris*, 140, 859-958.
- VOLSCHENK, E., S. 2005: A new technique for examining surface morphosculpture of scorpions. *Journal of Arachnology* 33, 820-825.
- VUKELIĆ, J., 2012: Šumska vegetacija Hrvatske (Forest vegetation of Croatia - in Croatian with large Summary in English). Sveučilište u Zagrebu, Šumarski fakultet, Državni zavod za zaštitu prirode, Zagreb, 403 pp.
- WATZ, M. & DUNLOP, J., 2022: Observations on regeneration of the pedipalp and legs of scorpions. *Euscorpius* 345, 1-5.